Int. J. Multiphase Flow, Vol. 2, pp. 261–272. Pergamon/Elsevier, 1975. Printed in Great Britain.

MEASUREMENTS OF VELOCITY, TEMPERATURE AND VELOCITY FLUCTUATION DISTRIBUTIONS IN FALLING LIQUID FILMS

T. UEDA and H. TANAKA
Department of Mechanical Engineering, University of Tokyo, Bunkyo-ku, Tokyo 113, Japan

(*Received* 16 *December* 1974)

Abstract—The velocity, temperature and velocity fluctuation distributions within falling spindle oil films in an inclined rectangular channel were measured using hot-wire techniques and thin thermocouples. The interfacial shear was caused by cocurrent air flow.

The results indicate that the liquid films are as a whole much more laminar-like than turbulent in a range of Reynolds numbers ($4\Gamma/\mu$) up to the experimental limit of 6000. Mixing motion occurs in the vicinity of the interface; however, the flow near the wall surface exhibits no sign of such eddy motions, as predicted by the wall law for single phase turbulent flow. Although velocity fluctuation is observed within films with interfacial shear, mean velocity profiles are approximately the same as those obtained by the laminar film prediction.

1. INTRODUCTION

A considerable amount of work has been performed to investigate the behaviour of liquid films in annular gas–liquid two-phase flow (for example Hewitt & Hall Taylor 1970; Ueda 1971), and many papers are devoted to studies on falling liquid films, dealing with average film thicknesses, wave characteristics, and various critical Reynolds numbers (Fulford 1964). Velocity distributions within liquid films, however, have been measured only in limited cases because of the difficulty arising from the fact that the liquid films normally encountered are very thin. Thus, the basic mechanism of heat and momentum transfer within the liquid films is still not well understood.

One of the authors conducted experiments on annular two-phase (air/water) flow in vertical tubes in which the interfacial shear stress, mean liquid film thickness, heat transfer coefficient, and thickness of the viscous sublayer of the liquid film were examined for both upflow and downflow (Ueda & Tanaka 1974; Ueda & Nose 1974). He also performed experiments on condensation of steam flowing downward in a vertical tube and investigated the behaviour of condensate films in the same manner (Ueda *et al.* 1972; Ueda *et al.* 1974). Results of these experiments suggested that liquid films in downflow are less turbulent than ones in upflow, and that downflow films are preserved in laminar state in a range of the Reynolds numbers up to about 1000, pass a very gradual transition to turbulent state with an increase of the Reynolds numbers from 1000 to 4000, and become the state in fair agreement with the prediction based on the wall law for single phase turbulent flow in a range of the Reynolds numbers higher than 4000. Several analytical predictions presented so far have been derived for liquid films in two-phase flow by applying the flow characteristics for the wall region of single phase flow. The above results of the author, however, reveal that downward films are as a whole retained in laminar-like state even in a range of the Reynolds numbers beyond those ever predicted.

As for falling liquid films, several investigators have measured average velocity distributions within the liquid films, with a goal of revealing the basic structure of liquid film flow. Wilke (1962) measured velocity and temperature profiles within liquid films falling on a vertical surface in laminar state. Ho & Hummel (1970) measured velocity distributions within falling liquid films inside a vertical Pyrex tube with a photochromic dye-tracer technique. Their experiments indicated no turbulent motion within liquid films even for the highest Reynolds number used, 2800. Isigai *et al.* (1971, 1973) estimated for their experiment on falling liquid films on a vertical surface, that the film flow was disturbed mainly by the breakdown of wave crests in a range of the Reynolds numbers up to 1600. Atkinson & Caruthers (1965) measured velocity profiles in a wide

range of Reynolds numbers by using hot-wire techniques for liquid film flow in a channel with very small angles of inclination. Their experimental profile for a Reynolds number 35000 agreed well with the prediction of the Deissler correlation, while velocity profiles for lower Reynolds numbers indicated a dependency on Reynolds number. Jeffries *et al.* (1969–1970) measured turbulence intensity in the vicinity of the interface.

Under existing circumstances, however, velocity profile measurements in a range of high Reynolds numbers are urgently needed to permit comparison with the wall law for single phase flow. In this study, thick liquid films are formed in an inclined rectangular channel using a spindle oil mixture as a test fluid, and velocity, temperature and velocity fluctuation distributions within the liquid films are measured with hot wire and thermocouple techniques for a range of Reynolds numbers from 3000 to 6000. Measurement of the temperature distributions is performed to detect the eddies within the films, since the Prandtl number of the test fluid is higher than 100 and hence the temperature distribution is very sensitive to the eddy motions.

2. OUTLINES OF THEORIES ON FILM FLOW

Theoretical treatment of film flow originated with Nusselt's (1916) theory for laminar liquid films. As for turbulent liquid films, Rohsenow *et al.* (1956) and Dukler (1960) presented ways of analysis by applying the wall law based on single phase flow to the film flow. Here, the existing theories will be outlined primarily along the lines of Duckler's analysis.

When a liquid of density ρ flows down a plate with inclination angle θ in the form of a thin film of thickness y_i with interfacial shear stress τ_i due to gas flow, a force balance for the whole film is

$$\tau_0 = \tau_i + \rho g \sin\theta \cdot y_i, \qquad [1]$$

where τ_0 is the shear stress at the wall surface (subscript $_0$ refers to the wall surface) and g the acceleration of gravity. Introducing a nondimensional mean film thickness, $y_i^* = y_i(g \sin\theta/\nu^2)^{1/3}$ (ν is the kinematic viscosity), and a nondimensional interfacial shear stress, $\tau_i^* = \tau_i/[\rho g \sin\theta\{\nu^2/(g \sin\theta)\}^{1/3}]$, and expressing the film thickness as $y_i\dagger = (y_i/\nu)\sqrt{\tau_0/\rho}$ in terms of a nondimensional length parameter of the wall law, [1] reduces to

$$(y_i\dagger)^2 = (y_i^*)^3 + \tau_i^*(y_i^*)^2. \qquad [2]$$

A force balance on the liquid layer at y from the wall becomes

$$\tau = \tau_0 - \rho g \sin\theta \cdot y. \qquad [3]$$

This is rewritten as

$$\frac{\tau}{\tau_0} = 1 - \left(\frac{y_i^*}{y_i\dagger}\right)^3 y\dagger, \qquad [4]$$

where

$$y\dagger = (y/\nu)\sqrt{\tau_0/\rho}.$$

The velocity gradient du/dy may be expressed as

$$\tau = \rho(\nu + \epsilon)\frac{du}{dy},$$

where ϵ is the eddy diffusivity for momentum. Therefore,

$$\frac{\tau}{\tau_0} = \left(1 + \frac{\epsilon}{\nu}\right)\frac{du\dagger}{dy\dagger}, \qquad [5]$$

where $u\dagger = u/\sqrt{\tau_0/\rho}$. For a laminar liquid film, $\epsilon = 0$. Then, substituting [4] into the left-hand side of [5] and integrating yields

$$u\dagger = y\dagger - \frac{1}{2}\left(\frac{y_i^*}{y_i\dagger}\right)^3 (y\dagger)^2. \qquad [6]$$

For a turbulent liquid film, the velocity gradient may be obtained by assuming the following expressions for the eddy diffusivity according to Deissler (1954):

$$\frac{\epsilon}{\nu} = n^2 u\dagger y\dagger \{1 - \exp(-n^2 u\dagger y\dagger)\} \quad \text{for} \quad 0 \leqq y\dagger < 26, \qquad [7]$$

and

$$\frac{\epsilon}{\nu} = \kappa^2 \left(\frac{du\dagger}{dy\dagger}\right)^3 \Big/ \left(\frac{d^2u\dagger}{dy\dagger^2}\right)^2 \quad \text{for} \quad 26 \leqq y\dagger, \qquad [8]$$

where $n = 0.109$ and $\kappa = 0.36$. Then, from [4] and [5] with the aid of [7] and [8],

$$[1 + n^2 u\dagger y\dagger \{1 - \exp(-n^2 u\dagger y\dagger)\}]\frac{du\dagger}{dy\dagger} = 1 - \left(\frac{y_i^*}{y_i\dagger}\right)^3 y\dagger \quad \text{for} \quad 0 \leqq y\dagger < 26, \qquad [9]$$

and

$$\frac{1}{\kappa}\frac{1}{\dfrac{du\dagger}{dy\dagger}} = 2\left(\frac{y_i\dagger}{y^*\dagger}\right)^3 \left[1 - \sqrt{\{1 - \left(\frac{y^*\dagger}{y_i\dagger}\right)^3 y\dagger\}}\right] \quad \text{for} \quad 26 \leqq y\dagger. \qquad [10]$$

Equation [10] is derived by neglecting the term of the unity due to molecular viscosity in [5] and by integrating once under the condition that $du\dagger/dy\dagger \to \infty$ as $y\dagger \to 0$. The numerical integration of [9] under the condition that $u\dagger = 0$ at $y\dagger = 0$ followed by the integration of [10] under the condition that $u\dagger$ is continuous at $y\dagger = 26$ results in the velocity profile of a turbulent film.

Integrating the velocity profile obtained above, the film Reynolds number defined by $Re_f = (4\Gamma/\mu)$ (Γ is the flow rate per unit width and μ the dynamic viscosity) can be determined and expressed in terms of $y_i\dagger$ and y_i^* as

$$Re_f = 4\int_0^{y_i\dagger} u\dagger dy\dagger. \qquad [11]$$

As for the four characteristic parameters of the liquid films, y_i^*, τ_i^*, $y_i\dagger$ and Re_f, when two of them (usually, Re_f and τ_i^*) are given, the other two are determined by [2] and [11]. Especially for a laminar liquid film, [6] can be easily integrated to yield Re_f with the aid of [2] as follows:

$$Re_f = 2(y_i\dagger)^2 - \frac{2}{3}(y_i^*)^3 = \frac{4}{3}(y_i^*)^3 + 2\tau_i^*(y_i^*)^2. \qquad [12]$$

The temperature gradient dt/dy may be expressed as

$$q = -\rho c_p \left(\frac{\nu}{Pr} + \epsilon_h\right)\frac{dt}{dy},$$

where q is the heat flux, ϵ_h is the eddy diffusivity for heat, and c_p and Pr respectively are the specific heat and the Prandtl number. Therefore,

$$\frac{q}{q_0} = \left(\frac{1}{Pr} + \frac{\epsilon_h}{\nu}\right)\frac{dt^\dagger}{dy^\dagger}, \qquad [13]$$

where $t^\dagger = \rho c_p (t_0 - t)\sqrt{\tau_0/\rho}/q_0$. Here, the turbulent Prandtl number is assumed to be $Pr_t = \epsilon/\epsilon_h = 1$. For the case of a fully developed liquid film which is heated at a uniform rate along the plate without evaporation and heat loss from the interface, the local heat flux q in the film varies as

$$\frac{q}{q_0} = 1 - \frac{\int_0^y u\,dy}{\int_0^{y_i} u\,dy} = 1 - \frac{4\int_0^{y^\dagger} u^\dagger dy^\dagger}{Re_f}. \qquad [14]$$

By substituting the velocity profile obtained previously into this equation and then substituting into the left-hand side of [13], the temperature distribution can be obtained by a numerical integration. For the case of a laminar liquid film without an interfacial shear, it becomes

$$t^\dagger = Pry^\dagger\left\{1 - \frac{1}{2}\left(\frac{y^\dagger}{y_i^\dagger}\right)^2 + \frac{1}{8}\left(\frac{y^\dagger}{y_i^\dagger}\right)^3\right\}. \qquad [15]$$

3. EXPERIMENTAL APPARATUS AND PROCEDURE

The test liquid used in the present study is a mixture of spindle oil and kerosene in a volume ratio of 87:13. Its physical properties are shown in figure 1. Figure 2 illustrates the experimental apparatus. The test liquid is maintained at a desired temperature in the storage tank and is pumped to an orifice flow meter and then to the test channel through a porous sinter section. After flowing down the channel, the liquid is separated from air and is cleared fairly scrupulously of bubbles before returning to the storage tank. Air enters through a smoothly contracting section

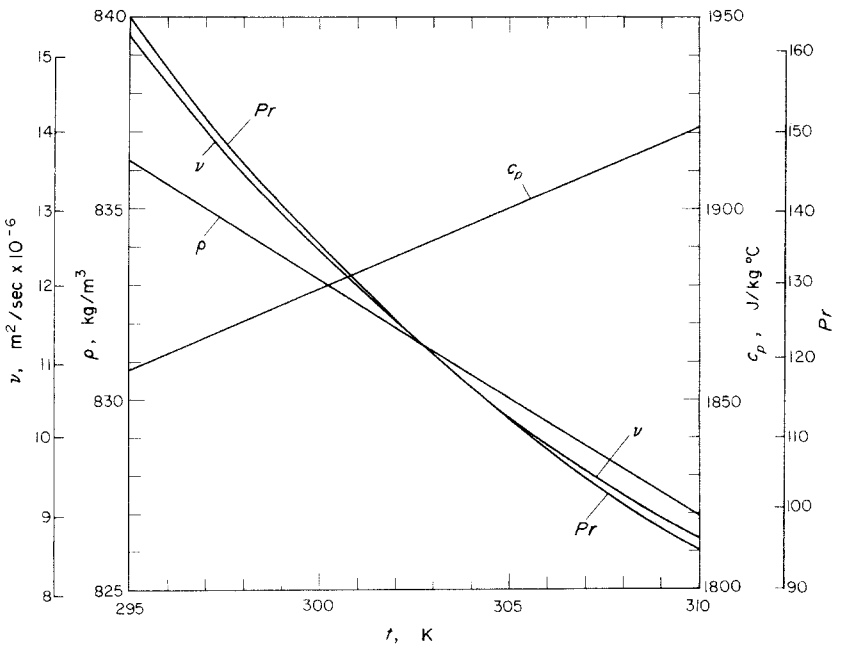

Figure 1. Variation of physical properties of test liquid against temperature t. Thermal conductivity $k = 0{\cdot}144$W/m°C nearly independent of temperature.

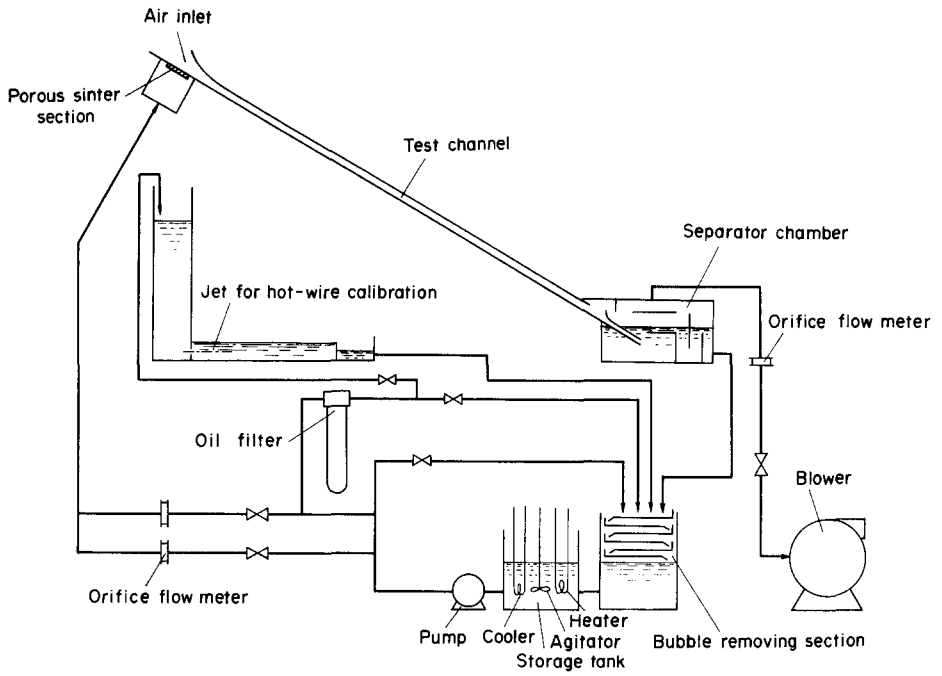

Figure 2. Experimental apparatus.

and flows in parallel with the liquid film. The air flow, separated from the liquid at the separator, is measured by an orifice flow meter and then goes to a blower.

The test channel made of transparent acrylic resin is 100 mm wide, 20 mm high and 2 m long, and is inclined at 40 degrees from the horizontal, figure 3. Pressure taps are located on the upper side wall at 850 mm and 1850 mm downstream of the lower limit of the porous section. A traversing mechanism, which is capable of setting a probe at exact distances from the under side wall is located 1700 mm downstream of the porous section. Either a hot-wire probe or a thermocouple probe was mounted to this mechanism, depending on the purpose of the test run. For isothermal runs, liquid temperature was measured at 30 mm downstream of the traversing station by a thermocouple. For the runs measuring temperature profiles, a 0.1 mm thick, 1 m long stainless steel plate fastened on the under side wall over the downstream half of the test channel was heated directly by passing an alternating current through it. The heating wall temperature was measured at 50 mm upstream of the traversing station by a thermocouple. The electrodes are attached to the side edges of the heating plate, as shown in figure 3 to minimize the disturbance

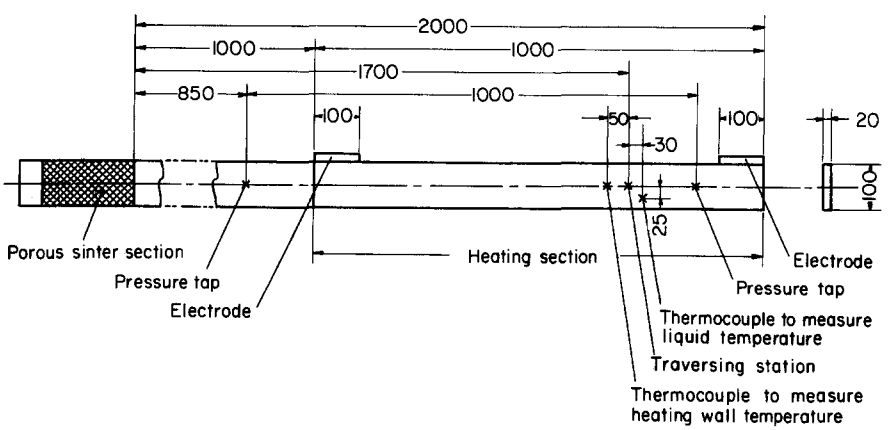

Figure 3. Test channel.

due to irregularities at the leading edge of the heating plate. In this arrangement, it was confirmed that heat flux was uniform except both regions of 200 mm from the leading and trailing edges.

Figure 4 illustrates the hot-wire probe used for measuring velocity and velocity fluctuation distributions. The probe was calibrated every day before and after the measurements by means of a jet effusing from an orifice under hydrostatic pressure (figure 2) to avoid errors due to change over a long period of time. The output character of the probe changed in a short term of a few tens of seconds, presumably owing to the deposition of small bubbles onto the hot-wire. The output change appeared most pronouncedly in stationary laminar flow, while it was moderated in flow with velocity fluctuation or turbulence. However, it was confirmed that the probe output always returned to the initial level immediately after a sudden velocity change. At the time of measurement, the probe suspended in the air flow was inserted into the fixed point in the film, and the output read without delay. Figure 5 shows the thermocouple probe used for temperature profile measurements.

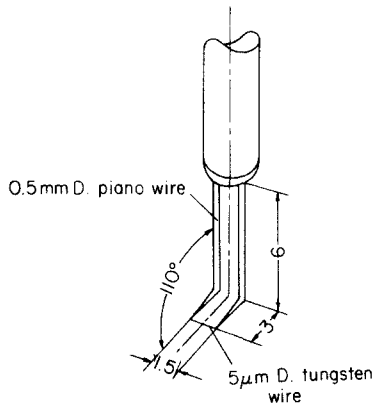

Figure 4. Hot-wire probe.

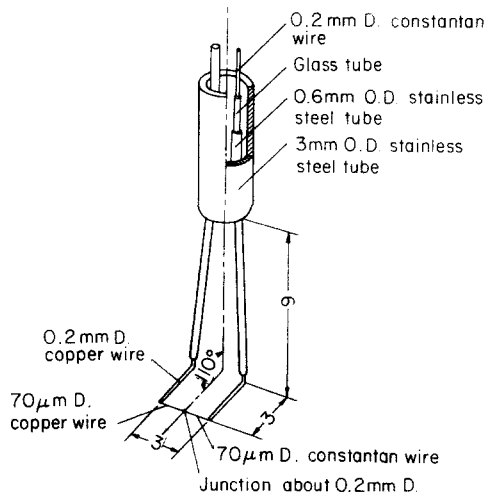

Figure 5. Thermocouple probe.

4. EXPERIMENTAL RESULTS

Figure 6 shows the measured velocities plotted against distance y from the wall for various air flow rates G_a under a constant volume flow rate of liquid Q_l. Each velocity profile has a sharp decrease near the interface, which may be attributed to intermittent exposure of the hot-wire to air flow at the troughs of waves. The interfacial shear stress τ_i was calculated from measured pressure gradient dp/dz, the channel height H and film thickness y_i by [16], in which the neutral plane of shear stress was assumed to coincide with the central plane of the air layer, since it was difficult to determine exactly the maximum point of air velocity profile in the experiment;

$$\tau_i = -\frac{dp}{dz}\frac{H - y_i}{2}. \qquad [16]$$

In this calculation, because of the difficulties in finding the mean film thickness of the wavy film, the film thickness was assumed as the distance y_i shown in figure 6 where the output decreased steeply. The shear stress τ_0 at the wall was determined from the velocity gradient near the wall. The velocity profiles were replotted using the non-dimensional parameters $u\dagger = u/\sqrt{\tau_0/\rho}$ and $y\dagger = (y/\nu)\sqrt{\tau_0/\rho}$ and are shown in figure 7. Various predictions from section 2 are also plotted in figure 7. Curve 1 represents the relation $u\dagger = y\dagger$ in the viscous sublayer. Curve 2 is Deissler's universal velocity profile for turbulent single phase flow. In the scope of this experiment, τ_i is so small as compared with τ_0 that the velocity profile computed by applying an actual value of $\tau_i{}^*$ scarcely differs from that assuming $\tau_i{}^* = 0$. Taking $\tau_i{}^* = 0$, [6] for laminar films was calculated to

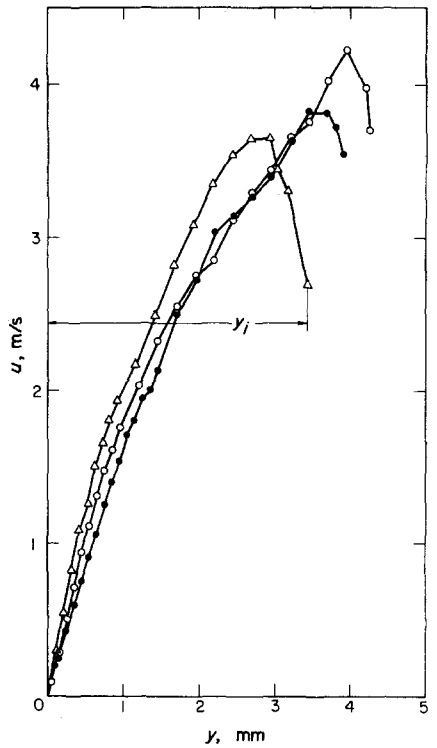

Figure 6. Velocity profile in liquid films. Keys are given in figure 7.

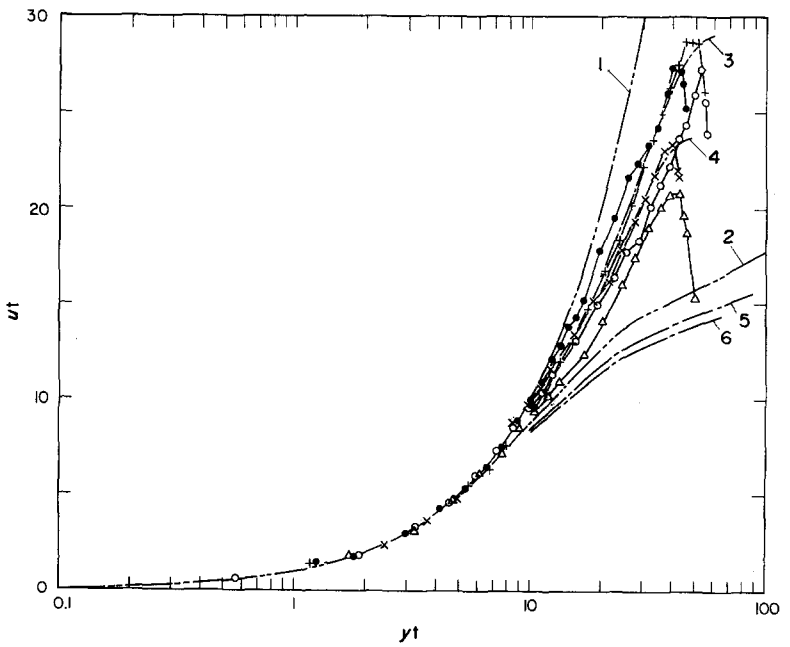

Figure 7. Comparison of measured velocity profiles with predicted values.

	Q_l(m³/hr)	G_a(kg/hr)	t(K)	Re_f	τ_0(N/m²)	τ_i(N/m²)	τ_i/τ_0	τ_i^*
○	4·80	60·2	301·6	4560	20·1	0·42	0·021	0·29
●	4·81	82·0	300·8	4420	16·5	1·1	0·065	0·72
△	4·80	100·5	300·8	4410	25·9	2·9	0·11	1·9
×	3·62	80·0	301·0	3350	18·0	0·95	0·053	0·64
+	6·00	76·0	301·6	5700	17·0	1·6	0·095	1·1

Curve 1: $u\dagger = y\dagger$. Curve 2: Deissler's prediction for turbulent full tube flow. Curve 3: Nusselt's prediction for laminar liquid film, $Re_f = 4500$, $\tau_i^* = 0$; Curve 4: $Re_f = 3000$, $\tau_i^* = 0$. Curve 5: Dukler's prediction for turbulent liquid film, $Re_f = 4500$, $\tau_i^* = 0$; Curve 6: $Re_f = 3000$. $\tau_i^* = 0$.

yield curves 3 and 4 corresponding to the experimental Reynolds numbers, and [9] and [10] for turbulent films were integrated to result in curves 5 and 6.

Velocity fluctuation distributions were measured simultaneously with velocity profiles. The results are shown in figures 8 and 9 as u'/u vs $y\dagger$ and $u'/\sqrt{\tau_0/\rho}$ vs $y\dagger$ respectively. In these figures, u' shows a sharp increase at large $y\dagger$, which may be attributed again to waves at the interface. Here, it should be noted that no velocity fluctuation was observed when the air flow

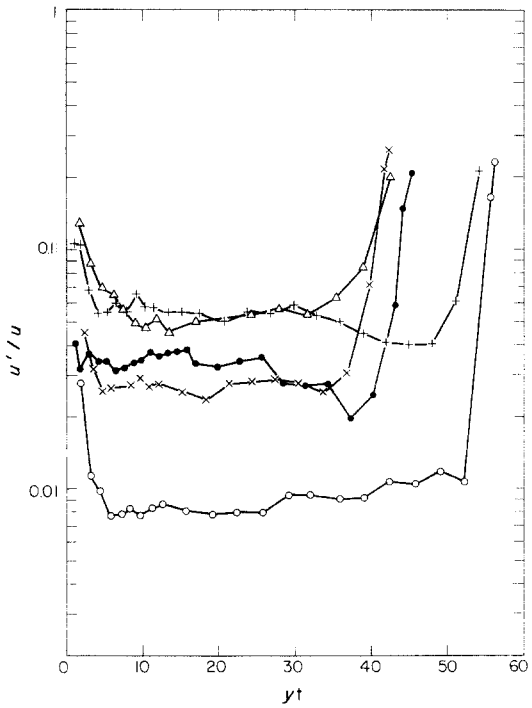

Figure 8. Distributions of velocity fluctuation. Keys are given in figure 7.

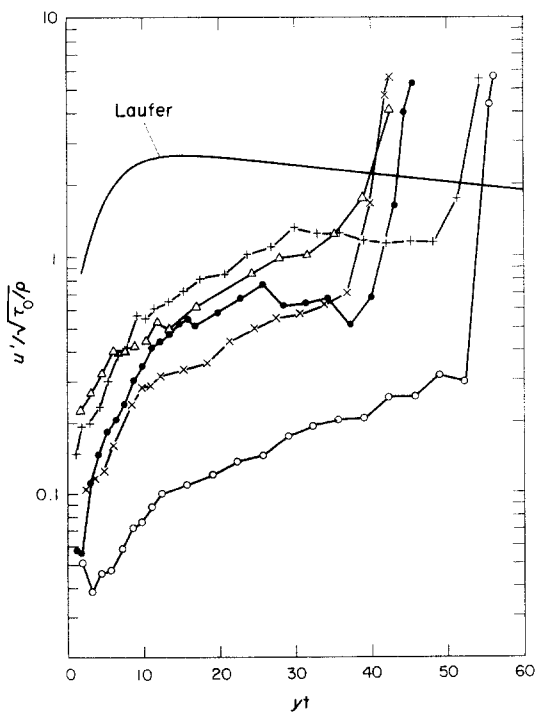

Figure 9. Distributions of velocity fluctuation. Keys are given in figure 7.

was stopped. In the case of turbulent boundary layers of single phase flow, a plot of $u'/\sqrt{\tau_0/\rho}$ against $y\dagger$ is considered to describe a universal curve irrespective of Reynolds numbers (Kudva & Sesonske 1972; Pennell *et al.* 1972). A typical curve is shown in figure 9 by the experimental result of Laufer (1954) for single phase flow.

For measurement of the temperature profile, a considerably smaller heat flux of $q_0 = 680\text{W/m}^2$ was imposed so as to restrain the temperature differences across liquid films within 3°C, lest the physical properties change extremely across the liquid films. In figure 10, the measured

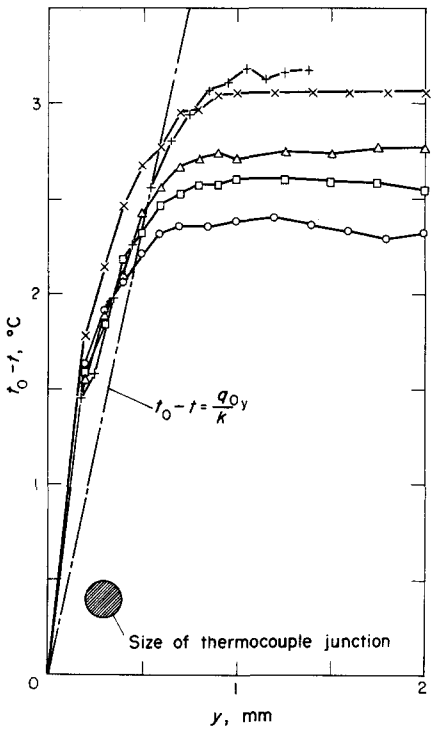

Figure 10. Temperature profile in liquid films. Keys are given in figure 11.

temperature drop from the wall, $t_0 - t$, is plotted against y. A dashed line in the figure represents the relation $t_0 - t = (q_0/k)y$ which holds if heat is transferred only by conduction. It is not surprising that the measured temperature profiles are over this dashed line in the range $y < 0.5$ mm since the thermocouple junction is about 0.2 mm in diameter. As the velocity gradient near the wall is very large, readings of thermocouple may be biased toward the value in the main stream. By using the physical properties at the film temperature $t_f = (t_0 + t_i)/2$, the temperature profiles were rearranged in the form of $t\dagger$ vs $y\dagger$ as shown in figure 11. In this figure, the data in the region $y < 0.5$ mm were omitted for the above reason. Prediction formulae described in section 2 are also plotted in figure 11. Curve 1 corresponds to the dashed line in figure 10. Curve 2 is Deissler's prediction for turbulent boundary layers of single phase fluid with a Prandtl number $Pr = 112$. Curve 3, corresponding to the measured profile denoted by the symbol +, represents the temperature profile in a laminar film given by [15]. When the film Reynolds number becomes slightly larger, the temperature profile in a laminar film almost coincides with curve 1 near the wall. Curve 4 for the case of $Re_f = 3000$, $Pr = 112$ and $\tau_i{}^* = 0$ was obtained from [9], [10], [13] and [14] for turbulent films, and differs only slightly from curve 2 for single phase flow.

5. DISCUSSION

For the velocity profiles in figure 7, it is noticeable that the liquid films seem to be much more laminar than turbulent, disagreeing with Dukler's predictions, up to the Reynolds number 5700. Further, the velocity profile is not strongly affected by the strength of the interfacial shear in this experimental range.

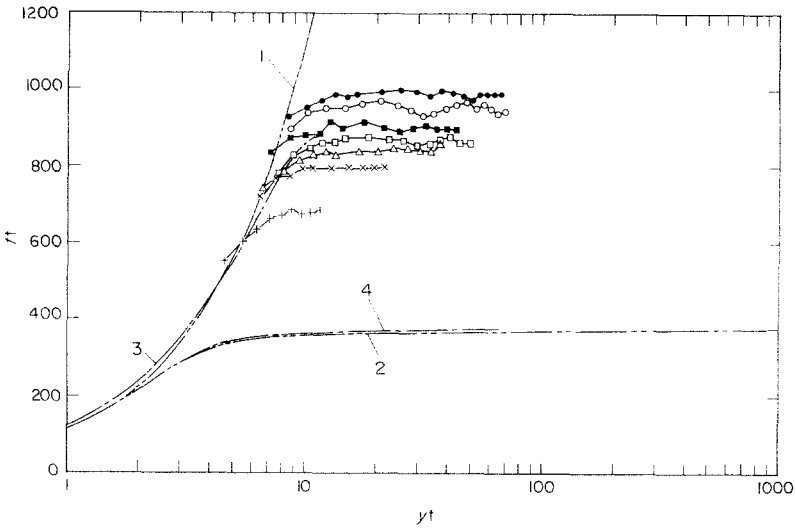

Figure 11. Comparison of measured temperature profiles with predicted values.

	Q_l(m³/hr)	G_a(kg/hr)	t_f(K)	Re_f	Pr_f	τ_l^*
+	0·18	0	303·1	180	121	0
×	0·60	0	304·7	640	114	0
△	1·20	0	306·5	1370	107	0
□	2·40	0	306·2	2710	108	0
■	2·40	80·0	304·5	2540	115	0·65
○	4·80	0	305·8	5350	110	0
●	4·80	80·0	304·3	5030	116	0·80

Curve 1: $t^\dagger = Pr \cdot y^\dagger$ (Pr = 112). Curve 2: Deissler's prediction for turbulent full tube flow (Pr = 112). Curve 3: Nusselt's prediction for laminar liquid film, Re_f = 180, Pr = 121, $\tau_l^* = 0$. Curve 4: Dukler's prediction for turbulent liquid film, Re_f = 3000, Pr = 112, $\tau_l^* = 0$.

The results of temperature profiles in figure 11 support the above knowledge about the velocity profiles. It is clear from [13] that eddy thermal conductivity becomes comparable to molecular thermal conductivity when $\epsilon_h/\nu = 1/Pr$. In the present experiment, $Pr \doteqdot 100$. Thus, curves 2 and 4 in figure 11, which assume the wall law for turbulent single phase flow, depart from curve 1 at about $y^\dagger = 2.5$ where the condition $\epsilon_h/\nu \doteqdot 1/100$ is fulfilled, and then become nearly horizontal for large $y^\dagger$. On the other hand, the data in figure 11 show no sign of such eddy diffusivity near the wall as predicted by the wall law, and indicate the existence of a thick molecular conduction layer. However, there must be some mixing motions at a distance from the wall, since the measured temperature profiles are horizontal for large $y^\dagger$. As the Prandtl number in this experiment is very high, even a slight eddy motion may flatten the temperature profile. Taking into account the fact that the velocity profiles approximately follow laminar predictions in figure 7, it may be concluded that the eddy diffusivity at a distance from the wall is of insignificant extent.

As shown in figures 8 and 9, considerable fluctuations of velocity have been observed in accordance with an increase of air flow rate. In this respect, the observed state of gas–liquid interface underwent the following changes. When the air flow rate G_a was 60 kg/hr, the interface was calm and smooth. As G_a was increased, there appeared several regions on the interface which looked white with swarms of small disturbance waves. The fraction of those white regions increased until G_a = 100 kg/hr, at which the whole interface waved furiously, splashing the upper side wall with droplets. The knowledge obtained from the velocity and temperature profiles suggests that the observed velocity fluctuations may be different in nature from those in turbulent boundary layers of single phase flow. This is supported by figure 9 in which the data of velocity fluctuations disagree with Laufer's universal profile. Here, it is noticeable in figure 8 that u'/u is nearly uniform despite the distance from the wall (except the neighbourhood of the interface) and

its value is approximately equal to (1/2) τ_i/τ_0. This fact might be explained by assuming the following mechanism of velocity fluctuations. The instantaneous strength of interfacial shear stress at any point may fluctuate around its mean value τ_i approximately by an amplitude $\tau_i/2$, owing to the turbulent motions in the air flow. Then, provided the liquid film is in laminar state, the mean velocity u is expressed as

$$u = \frac{1}{\mu}\left[\rho g \sin\theta\left(y_i y - \frac{y^2}{2}\right) + \tau_i y\right] = \frac{y}{\mu}\left[(\tau_0 - \tau_i)\left(1 - \frac{y}{2y_i}\right) + \tau_i\right] \doteqdot \frac{\tau_0}{\mu} y\left(1 - \frac{y}{2y_i}\right),$$

and the velocity fluctuation caused by the interfacial shear variation of $\tau_i/2$ may have an amplitude of $u' = (1/2)(\tau_i/\mu)y$. In consequence, $u'/u \sim (1/2)\tau_i/\tau_0$. Then, although some eddies exist at a distance from the wall, the major part of the velocity fluctuation is considered to be the laminar fluctuation due to the interfacial shear variation.

The above discussions support qualitatively our previous experimental results on liquid films of annular two-phase flow in vertical tubes mentioned in the introduction. Further increasing of the interfacial shear or the film Reynolds number will bring about an increase of eddy motions in the films and spreading of an eddy predominant layer, and will transform the film flow into fully turbulent state. In the present experiment, however, a developed turbulent state was not observed, nevertheless measurements were performed up to Reynolds numbers comparable to those where vertical liquid films had become fully turbulent in previous experiments. This may be attributed to the gravity component normal to the wall acting upon liquid films on an inclined plate to suppress growing up of wave motion and breakdown of wave crests.

6. CONCLUDING REMARKS

The velocity, temperature and velocity fluctuation distributions within liquid films on an inclined plate were measured in a range of Reynolds number Re_f to 6000 and the interfacial shear τ_i^* to 2. On the basis of the results the following conclusions were reached.

(i) There are some mixing motions at a distance from the wall; however, the flow near the wall surface is accompanied with no sign of such eddy motions as predicted by the wall law for single phase turbulent flow.

(ii) When the interfacial shear is generated by cocurrent air flow, the velocity fluctuation is observed within the film. This seems to be caused by the fluctuation of the interfacial shear. In the present experimental range, however, this velocity fluctuation does not yield such mixing motions as eddies in developed turbulent flow do, and the mean velocity profiles are approximately the same as those obtained by the laminar film prediction.

Acknowledgement—The authors wish to acknowledge the assistance of Mr. Tomohiro Shibuya, Mr. Hiroyuki Matsui and Mr. Kenji Ishida in many parts of this study.

REFERENCES

ATKINSON, B. & CARUTHERS, P. A. 1965 Velocity profile measurements in liquid films. *Trans. Instn Chem Engrs* **43**, T33–39.

DEISSLER, R. G. 1954 Heat transfer and fluid friction for fully developed turbulent flow of air and supercritical water with variable fluid properties. *Trans. Am. Soc. Mech. Engrs* **76**, 73–85.

DUKLER, A. E. 1960 Fluid mechanics and heat transfer in vertical falling-film system. *Chem. Engng Prog. Symp. Ser.* **56-30**, 1–10.

FULFORD, G. D. 1964 The flow of liquids in thin films *Adv. Chem. Engng* **5**, 151–236.

HEWITT, G. F. & HALL TAYLOR, N. S. 1970 *Annular Two-Phase Flow.* Pergamon Press.

HO, F. C. K. & HUMMEL, R. L. 1970 Average velocity distributions within falling liquid films. *Chem. Engng Sci.* **25**, 1225–1237.

ISIGAI, S., NAKANISHI, S., KOIZUMI, T. & OYABU, Z. 1971 Hydrodynamics and heat transfer of vertical

falling liquid films, Part 1, Classification of flow regimes. *Trans. Japan Soc. Mech. Engrs* **37**, 1708–1715.

ISIGAI, S., NAKANISHI, S., TAKEHARA, M. & OYABU, Z. 1973 Hydrodynamics and heat transfer of vertical falling liquid films, Part 2, Analysis by using heat transfer data. *Trans. Japan Soc. Mech. Engrs* **39**, 1620–1627.

JEFFRIES, R. B., SCOTT, D. S. & RHODES, E. 1969–1970 Structure of turbulence close to the interface in the liquid phase of a co-current stratified two-phase flow. *Proc. Instn Mech. Engrs* **184**-Pt3C, 204–214.

KUDVA, A. K. & SESONSKE, A. 1972 Structure of turbulent velocity and temperature fields in ethylene glycol pipe flow at low Reynolds number. *Int. J. Heat Mass Transfer* **15**, 127–145.

LAUFER, J. 1954 The Structure of Turbulence in Fully Developed Pipe Flow. NACA TR 1174.

NUSSELT, W. 1916 Die Oberflächenkondensation des Wasserdamphes. *Z. Ver Dt. Ing.* **60**, 541–546.

PENNELL, W. T., SPARROW, E. M. & ECKERT, E. R. G. 1972 Turbulence intensity and time-mean velocity distributions in low Reynolds number turbulent pipe flows. *Int. J. Heat Mass Transfer* **15**, 1067–1074.

ROHSENOW, W. M., WEBER, J. H. & LING, A. T. 1956 Effect of vapor velocity on laminar and turbulent-film condensation. *Trans. Am. Soc. Mech. Engrs* **78**, 1637–1643.

UEDA, T. 1971 A review of two-phase (gas–liquid) flow. *J. Japan Soc. Mech. Engrs* **74**, 523–532.

UEDA, T., AKIYOSHI, K., MATSUI, T. & INQUE, M. 1972 Heat transfer and pressure drop for flow condensation inside a vertical tube. *Bull. Japan Soc. Mech. Engrs* **15**, 1267–1277.

UEDA, T. & TANAKA, T. 1974 Studies of liquid film flow in two-phase annular and annular-mist flow regions, Part 1, Downflow in a vertical tube. *Bull. Japan Soc. Mech. Engrs* **17**, 603–613.

UEDA, T. & NOSE, S. 1974 Studies of liquid film flow in two-phase annular and annular-mist flow regions, Part 2, Upflow in a vertical tube. *Bull. Japan Soc. Mech. Engrs* **17**, 614–624.

UEDA, T., KUBO, T. & INQUE, M. 1974 Heat transfer for steam condensing inside a vertical tube. *Proc. 5th Int. Heat Transfer Conf.*, Tokyo, Vol. 3, 304–308.

WILKE, W. 1962 Wärmeübertragung an Rieselfilme. VDI-Forsch.-h. 490, B-28.

Résumé—On a mesuré avec des techniques de fil chaud et des thermocouples fins, les distributions de vitesse, température et fluctuation de vitesse dans des films d'huile spindle descendants dans des canaux rectangulaires inclinés. La contrainte interfaciale était imposée par un écoulement co-courant d'air.

Les résultats indiquent que les films liquides se comportent dans l'ensemble beaucoup plus comme laminaires que comme turbulents dans une gamme de nombres de Reynolds ($4\Gamma/\mu$) atteignent 6000. Il y a quelques mouvements de mélange au voisinage de l'interface; cependant l'écoulement près de la paroi ne montre aucun signe des mouvements tourbillonnaires prévus à partir de la loi à la paroi pour les écoulements turbulents monophasiques. Bien que des fluctuations de vitesse soient observées au sein des films soumis à une contrainte interfaciale, les profils de vitesse moyenne sont approximativement les mêmes que ceux qui résultent des prévisions pour un film laminaire.

Auszug—Die Verteilung von Geschwindigkeit, Temperatur und Geschwindigkeits-schwankungen in Spindeloelschichten, die in geneigten rechteckigen Kanaelen abwaertsstroemen, wurde mittels Hitzdrahtanemometer und duenner Thermoelemente gemessen. Schubspannungen in der Grenzflaeche wurden durch parallele Luftstroemung eingestellt. Die Ergebnisse zeigen Fluessigkeitsschichten, die im grossen Ganzen viel mehr laminarer als turbulenter Stroemung aehneln, bei Reynoldschen Zahlen ($4\Gamma/\mu$) bis zur Versuchsgrenze von 6000. Waehrend sich in der Naehe der Grenzflaeche einige Mischvorgaenge abspielen, sind in der wandnahen Stroemung keine solchen Wirbelbewegungen, wie sie das Wandgesetz der turbulenten Einphasenstroemung vorhersagt, wahrnehmbar. Trotzdem in den Schichten mit Grenzflaechenschub Geschwindigkeitsschwankungen gemessen werden, ergeben sich die mittleren Geschwindigkeitsprofile annaehernd wie durch die laminare Schichttheorie vorhergesagt.

Резюме—С помощью нагретых проволочек и тонких термопар измерялись распределения скоростей, температур и флуктуаций скоростей в тонких пленках веретенного масла, стекающих в наклонных прямоугольных каналах. Межфазный сдвиг задавался прямотоком воздуха. Результаты показывают, что в общем жидкие пленки значительно более подобны ламинарным, чем турбулентным при изменении критерия Рейнольдса ($4\Gamma/\mu$) на экспериментальной границе до 6000. Существуют некоторые смешивающие перемещения вблизи указанной межфазной границы, однако поток вблиеи пристеночной поверхности не сопровождается никакими следами вихревых движений, как это предсказывается законом стенки для однофазного турбулентного течения. Хотя и внутри пленок с поверхностным сдвигом были наблюдены флуктуации скоростей, профили средних скоростей соответствовали профилям, ожидаемым для ламинарных пленок.